



Sensitivity analysis of wind turbine fatigue reliability: effects of design turbulence and the Wöhler exponent

Shadan Mozafari^{1,*}, Paul Veers², Jennifer Marie Rinker¹, and Katherine Dykes¹

¹Department of Wind Energy, Technical University of Denmark, Roskilde, Denmark

²National Renewable Energy Laboratory (NREL), Golden, CO, USA.

Correspondence: Shadan Mozafari (Shad.mzf@gmail.com)

Abstract.

Fatigue reliability assessment of wind turbine components involves three major sources of uncertainty: material resistance, loads, and the mathematical models that connect the other two. Many studies focus on decreasing the uncertainty in fatigue load assessments via different approaches including more detailed characterization of the turbulence standard deviation (turbulence) in the design phase. The IEC standard suggests two different distributions in Edition 3 and Edition 4 as alternatives for the representative turbulence in its Normal Turbulence Model (NTM): lognormal and Weibull. There are debates on whether the two suggested distributions provide adequately safe reliability in relevant load channels since the established design safety factors are calibrated based on the representative turbulence approach. The current study addresses the debate by comparing annual reliability based on different scenarios of NTM using a probabilistic approach. More importantly, it elaborates on the level of importance of this matter or most of the other concerns about the load's uncertainty in the context of reliability considering all uncertainty in the material properties and the linear damage accumulation rule.

Using aeroelastic simulations of the DTU 10MW reference wind turbine and a simple model for assessing fatigue reliability based on the distribution of damage equivalent load (DEL), we study the changes and the trends in the annual reliability as well as the relative importance of each of the uncertainty groups. In addition, we investigate the effects of different fatigue exponents on the overall results in the blade root flapwise and the tower base fore-aft load channels.

The results show that generally using the distribution of turbulence in each mean wind speed results in less conservative annual reliability levels compared to representative turbulence. The difference in the reliability levels varies according to turbulence distribution and the fatigue exponent. In the case of the tower base, the difference in reliability after 20 years can be up to 50%. However, the model and material uncertainty have much higher effects on the reliability levels compared to DEL uncertainty. Knowledge about such differences in the reliability levels due to the choice of turbulence characterization method is especially important as it impacts the extent of lifetime extension through reliability re-assessments.

keywords: Wind turbine reliability, Fatigue reliability, Uncertainty quantification, Sensitivity analysis, Normal Turbulence Model, Turbulence distribution



1 Introduction

25 The fatigue reliability of a structure is its ability to withstand cyclic loading during the design lifetime. Fatigue life is a highly sensitive and uncertain variable (Veers, 1996). In the case of wind turbines, the random and variable amplitude loading and the complexity of the structural system increase such uncertainty. In addition, there is a high level of uncertainty in material strength data and the simplified models commonly used for counting cycles or describing the material properties and damage accumulation. The probabilistic approach for fatigue reliability assessment involves probabilistic modeling of the crucial random inputs leading to a more robust analysis and design of the wind turbines against fatigue (Choi et al., 2007). The IEC design standard introduces a semi-deterministic approach that includes safety factors to account for the uncertainty in different inputs. These factors are calibrated based on probabilistic reliability assessment aiming at an acceptable target reliability level at the end of operation time (design lifetime). It is clear that the uncertainty analysis of the mentioned sources is an important part of the probabilistic reliability assessment. Fig. 1 shows the general schematic view of the main random inputs of the fatigue reliability assessment considered in the current study.

35

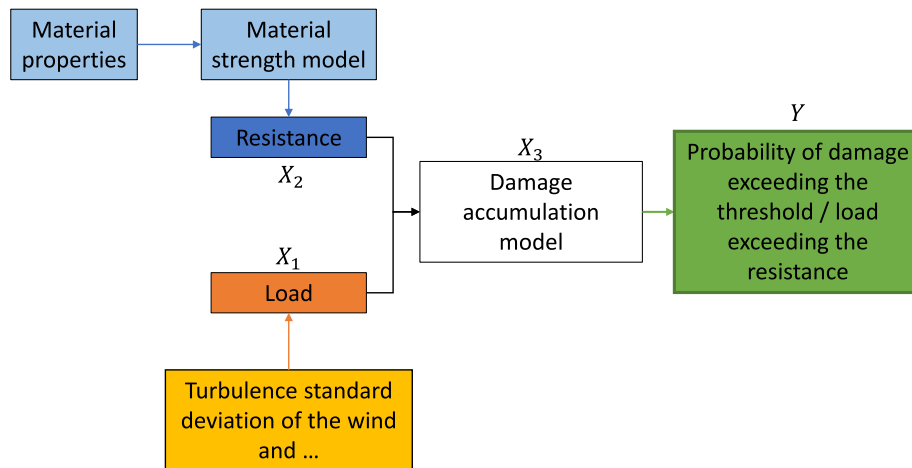


Figure 1. Flowchart of the main random inputs (X_i) and the output (Y) in the fatigue reliability assessment

Stensgaard et al. (2016a) show that wind climate parameters contribute to about 10%–30% of the total uncertainty in the reliability estimation. Furthermore, the sensitivity analysis results in (Stensgaard et al., 2016a; Dimitrov et al., 2018; Robertson et al., 2019; Murcia et al., 2018) reveal that after the mean wind speed, the standard deviation of the wind (turbulence) has the largest impact on the equivalent fatigue load levels in most of the load channels. Thus, accurate modeling of the turbulence at the design level is crucial for decreasing the uncertainties in the fatigue loads.

40



The IEC standard (IEC 61400-1, 2005) suggests the Normal turbulence model. The model is mainly based on a representative value in each wind speed bin for estimating turbulence. The representative value is the 90% quantile of a lognormal distribution. However, the standard also keeps the option of using the whole distribution open for the designer. Edition 4 of the IEC standard (IEC 61400-1, 2019) suggests a Weibull distribution with the same 90% quantile magnitude.

There are some studies investigating the performance of the different approaches of NTM in describing the site turbulence conditions. For example, Ren et al. (2018) investigated the compatibility of 90% quantile recommendation for describing onshore conditions and showed that it overestimates the turbulence. Thus, they proposed a three-parameter power-law model for turbulence intensity. In addition, Øistad (2015) investigated the performance of representative turbulence recommendations on a case with both onshore and offshore wind conditions and concluded that the model overestimates the turbulence levels in both cases. There are more similar studies focusing on offshore conditions (Wang et al., 2014; Türk and Emeis, 2010; Tsugawa et al., 2015) showing the inaccuracy of the IEC standard recommendations compared to real wind fields. In addition, Ishihara (2012) presents the same results by studying the compliance of the lognormal distribution of the IEC standard with measurements in an offshore wind farm. As another example, Dimitrov et al. (2017) show that for their case study site, the lognormal distribution provides over-conservative turbulence expectations and thus, suggests 2-parameter Weibull distribution. The results of (Søndergaard and Jóhannsson, 2016) also conclude lognormal to be conservative. They suggested Weibull distribution as a better (less conservative choice) in the case of blade fatigue and extreme loads. Emies (2014) shows an offshore case within which the IEC Normal turbulence model provides under-conservative results for turbulence intensity in low mean wind speeds and over-conservative values in higher mean wind speeds. A few studies like (Larsen, 2001; Wang et al., 2014) explicitly introduce other approaches for modeling offshore turbulence as they propose that the Normal turbulence model of the IEC standard is over-conservative for all offshore cases.

In addition, there are some studies on the loads corresponding to each turbulence characterization approach. The results of these studies vary from each other. For example, some pieces of research like (Ernst et al., 2012; Dimitrov et al., 2017; Hansen and Larsen, 2005) show that the IEC representative and lognormal turbulence models are very conservative in the case of blade loads and propose new, less conservative turbulence models. On the other hand, the results of (Stensgaard et al., 2016a) show that following the suggestion on 90% quantile level for turbulence in the IEC standard leads to an accurate assessment of the blade root flapwise bending moment while producing a conservative assessment of the tower bottom fore-aft bending moment and low-speed shaft torque. It has to be noted that these comparisons are done with real data in which the wind shear is also variable (and a function of turbulence) and it can greatly affect special load channels.

As a second matter, the effect of uncertainty in the material properties on fatigue reliability assessment is also covered in many studies. According to previous research, like (Veers, 1996; Zaccone, 2001), the uncertainty inherent in the material properties including physical, modeling, and measurement uncertainty represent almost half the total uncertainty. The results of the sensitivity analysis in (Velarde et al., 2020)) and (Ronold et al., 1999) show that the uncertainties related to the material resis-



80 tance model have the highest influence on fatigue reliability. Bacharoudis et al. (2015) presented the high sensitivity of wind turbine blade reliability to the measurement uncertainty in the material properties of the composites using the DTU 10-MW wind turbine as the case study.

85 All in all, there are many studies on the level of accuracy and performance of the representative turbulence suggestion and they all show the need for transition from such a model to lognormal and Weibull distributions especially in the case of offshore wind farms with lower turbulence levels. However, they have not compared different scenarios to each other in general design conditions and it is still under debate if the two distributions always provide safe reliability levels for different load channels. The current work addresses this gap and such debate. Knowing the difference between the reliability levels when following different NTM approaches is especially important because the established safety factors for the semi-deterministic approach in the IEC design standard are calibrated based on the representative turbulence approach. Thus, one should be aware that if they assess the reliability levels using the same safety factors while characterizing the standard deviation turbulence by distribution, the semi-deterministic approach and probabilistic approach do not meet at the same reliability level at the end of the component's design lifetime. It is important to make sure that the two alternative distributions are never under-conservative. Furthermore, having information about the level of differences can be an asset for fast initial estimation of the possible extension of a lifetime only by knowledge about the considered approach in the design phase. It is clear that such information about the design assumptions is also crucial in the more detailed assessments of lifetime extension using site-specific data.

95

In addition, considering the results of the previous studies on the importance of material uncertainty in fatigue reliability, it is valuable to study how all the efforts for accurate characterization of the turbulence will transfer to a more accurate reliability assessment considering the high uncertainty in material properties and model. In the present study, we reveal how different approaches in the IEC standard for a general case can change the distribution of the fatigue loads. In addition, we study the sensitivity of the reliability to the change in the fatigue load compared to its sensitivity to other random inputs.

105 The results of the current study cover blade flapwise and tower base fore-aft load channels in a large wind turbine (10-MW) from IEC class 1A. We study the differences in distributions of DEL in different suggestions of the IEC standard regarding turbulence using a large number of aeroelastic simulations and bootstrapping. In addition, the results show the relative importance of DEL variation due to turbulence by comparing its effect with two other major sources of uncertainty in the fatigue reliability assessment. The knowledge about the importance factors is a guide for designers and researchers showing where they should put their focus and efforts regarding reducing uncertainty to get more robust reliability levels. The fatigue exponent is the exponent to which the load is powered in the damage models commonly used (as in the current study). Thus, it directly changes the share of the loads in the fatigue damage. This parameter also changes the distribution of DEL (Mozafari et al., 2023), thus, we also investigate the results of the reliability study in different fatigue exponent levels in each load channel. An important note is that since the DTU 10-MW turbine is not designed against fatigue, we observed low-reliability levels in the blade root and the tower base, and thus the mean value of the material properties are scaled and the reliability levels are



not based on real data. In other words, the trends and effects which are the purpose of the current study are reliable but the reliability levels are not.

115

In the following sections, first, we provide information about the wind turbine case study in Sect. 2.1 and the characteristics of the aeroelastic simulations in Sect. 2.2. In addition, Sect. 3.1 provides information about the assumptions and the mathematical relations used in the current study for assessing fatigue loads, post-processing simulation results as well as reliability assessment and sensitivity analysis methods. Then, Sect. 3 presents the results in three parts: Sect. 3.1 covers the results of DEL distributions, Sect. 3.2 shows the results of the reliability assessments and Sect. 3.3 provides the sensitivity analysis of the reliability. Finally, Sect. 4 contains the conclusions of the study, limitations, and suggestions for future research in the area.

120

2 Methodology

We use 10-minute aeroelastic simulations to obtain the load time series and estimate the fatigue reliability based on them. Sect. 2.1 explains the specifications of the case study wind turbine and Sect. 2.2 introduces the properties of the simulations. Finally, Sect. 2.3 explains the mathematical relations and methods we use.

125

2.1 The case study wind turbine

We consider the DTU 10MW reference wind turbine (Bak et al., 2013) as our case study. The DTU 10MW is an offshore wind turbine from IEC standard class 1A (IEC 61400-1, 2019) with a rotor diameter of 178.3 meters and a hub height of 119 meters. It is rated at a power of 10 MW and a mean wind speed of 11.4 m/s. The cut-in and cut-out mean wind speeds are 4 m/s and 26 m/s, respectively. The blade in the current case study is made of unidirectional E-glass fiber epoxy and the tower is made of steel.

130

2.2 Aeroelastic simulations

We perform three groups of simulations, representing three case studies, forming a total of 98400 10-minute aeroelastic simulations of the DTU 10-MW reference wind turbine in HAWC2¹ software (Larsen and Hansen, 2007). The difference between the three groups lies in the modeling of turbulence (standard deviation of wind) in different wind speed levels. Although fatigue can occur in different conditions, in the current work, we only consider operational conditions and not the fatigue damage due to the start-up or shutdown events for simplicity. Thus, we perform the simulations based on IEC standard DLC 1.2 load case (IEC 61400-1, 2019) with Normal wind conditions. As another simplification, we set the wind direction constant and equal to zero in all the simulations. The mean wind speed (MWS) varies from 4 m/s (cut-in) to 26 m/s (cut-out) in bins of size 2 m/s. We use the Mann turbulence model, which is a method for simulation of the wind field (see (Mann, 1998)), for generating the turbulence boxes in the simulations. The boxes contain 8192 evaluation points in the wind direction for higher resolution

140

¹An aeroelastic code for calculating wind turbine response in the time domain- developed in DTU Wind energy department between years 2003-2007



and 32 points in each of the other two perpendicular directions. Each wind bin (a combination of wind speed and turbulence) consists of 200 turbulence realizations. Table 1 presents the specifications of wind load modeling in each group of simulations.

Table 1. Specifications of wind modeling in three groups of HAWC2 simulations corresponding to three study cases

Parameter	Group 1	Group 2	Group 3
Marginal distribution of turbulence	constant	Log-normal	Weibull
Turbulence levels in each MWS bin	1	20	20
Realizations per wind condition	200		
Wind shear exponent	0.2		
Turbulence model	Mann		
Cut-in mean wind speed (<i>m/s</i>)	4		
Cut-out mean wind speed (<i>m/s</i>)	26		
Rated wind speed (<i>m/s</i>)	11.4		
Size of wind speed bins (<i>m/s</i>)	2		
Mean wind speed distribution	Rayleigh		
Yaw angle (degrees)	0		
Mann box grids along the wind	8192		
Mann box grids in other dimensions	32		
Time steps of the simulations (sec.)	0.01		

We consider the flapwise bending moment in the blade and the fore-aft bending moment in the tower base as the main 145 outputs of the simulations and the input for the fatigue assessment of the blade and tower base.

2.3 Mathematical formulations

In the following, we present the mathematical background and relations that we use to post-process simulation load outputs and estimate the corresponding fatigue damage and reliability.

2.3.1 Probabilistic modeling of wind

150 The wind as a random process is mostly described by its mean value and standard deviation (turbulence) at each point of time and space. The IEC standard (IEC 61400-1, 2019) presents a Rayleigh distribution for probabilistic modeling of the mean wind speed at the wind turbine’s hub height. Eq. (1) presents the cumulative distribution function (CDF) of the mean wind speed based on the suggested Rayleigh distribution.

$$F(V_{hub}) = 1 - \exp\left(-\pi\left(\frac{V_{hub}}{2V_{ave}}\right)^2\right) \quad (1)$$



155 In Eq. (1), $F(V_{hub})$ is the CDF. Furthermore, v_{hub} accounts for the mean wind speed at the hub height and v_{ave} is the annual mean wind speed at the hub height. In the standard wind turbine classes $v_{ave} = 0.2v_{ref}$ in which the v_{ref} is the 50-year extreme wind speed over 10 minutes. The parameter v_{ref} is equal to 50 m/s in the IEC class 1 category (IEC 61400-1, 2019) which is the class of the current case study wind turbine.

The statistical parameters of the wind are correlated. In other words, the standard deviation of the wind changes with a
160 change in the mean level. However, since the IEC design standard suggests binning of the wind speeds (as we do in our simulations), one can use the marginal distribution of turbulence in each wind speed bin. The third edition of the IEC standard (IEC 61400-1, 2005) presents a lognormal distribution as the marginal distribution of turbulence within each wind speed level. The fourth edition (IEC 61400-1, 2019) suggests Weibull distribution. Following each of the distributions, the designer is provided with two options in the IEC standards. The first option is to consider the constant representative turbulence for each
165 wind speed bin, equal to 90% quantile of the distribution, instead of the marginal distribution. The other option is to consider the whole distribution domain in each wind speed bin.

The current study investigates the impact of NTM turbulence characterization choice on design fatigue reliability as it has not been studied before. For this purpose, we define three cases for the different turbulence characterization approaches: case 1 covers the 90% quantile turbulence value, and cases 2 and 3 refer to the lognormal and Weibull distributions, respectively.
170 Equation (2) and Eq. (3) show the standard deviation and mean of turbulence of the suggested lognormal distribution, respectively (case 2). In addition, Eq. (4) shows the 90% quantile value of the same distribution (case 1).

$$\sigma_T = \sqrt{\ln\left(\frac{(I_{ref})^2}{0.75V_{hub} + 3.8} + 1\right)} \quad (2)$$

$$\mu_T = \ln(TI_{ref}(0.75V_{hub} + 3.8)) - \frac{(\sigma_T)^2}{2} \quad (3)$$

$$T_{rep.} = I_{ref}(0.75v_{hub} + 5.6) \quad (4)$$

175 In Eq. (2) to Eq. (4), I_{ref} is the reference turbulence intensity equal to 0.16 for the standard class 1 wind turbines (the current case study). In addition, μ_T and σ_T are the mean and standard deviation of the turbulence as a function of the hub height wind speed (V_{hub}) and $T_{rep.}$ is the representative turbulence equal to 90% quantile of the lognormal distribution.

Equation (5) and Eq. (6) present the shape and scale parameters of the Weibull distribution which the fourth edition of the IEC standard (IEC 61400-1, 2019) suggests.

$$180 \quad k = I_{ref}(0.27v_{hub} + 1.4) \quad (5)$$

$$C = I_{ref}(0.75v_{hub} + 3.3) \quad (6)$$

In Eq. (5) and (6), k and C represent the shape and scale parameters of the Weibull distribution, respectively. Weibull is a very flexible distribution and can be close to many other distributions including lognormal depending on its shape parameter. Fig. 2 presents the cumulative probability distributions of cases 2 and 3 in one mean wind speed of 8 m/s.

185

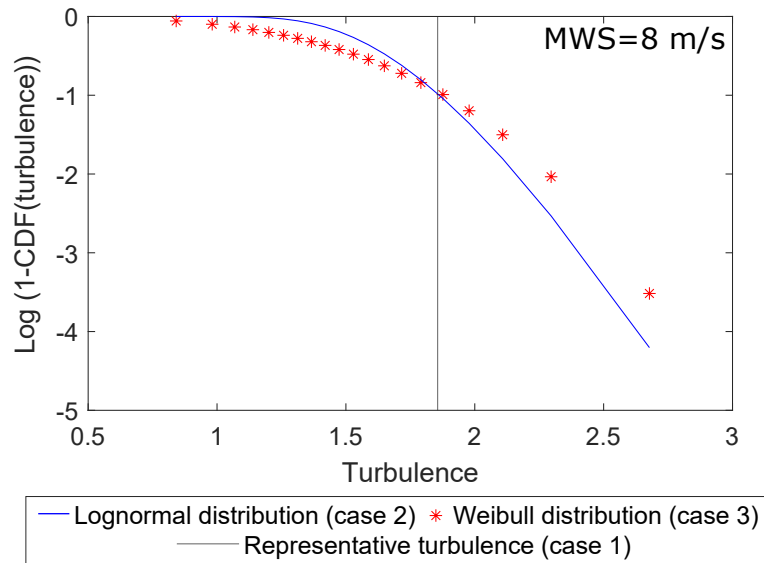


Figure 2. lognormal and Weibull distribution of turbulence at 8 m/s compared to the 90% quantile level (representative turbulence level)

The lognormal distribution is generally heavy-tailed and as Fig. 2 shows it has a thicker tail compared to the Weibull distribution in the example. In other words, with the same accumulated probability in the tail (for example the 10% upper tail), the lognormal tail covers lower turbulence levels than the Weibull distribution. The thin tail of the Weibull distribution and relatively lower mean value (as seen in Fig. 2) also leads to high standard deviations. All in all, the two distributions have opposite behaviors in the two portions before and after their intersection at 90% quantile. The Weibull distribution represents higher probabilities in the lower turbulence levels and covers more data from lower values considering the same number of observations. Therefore, in general, we expect using the Weibull distribution for representing the occurrences of turbulence to be a less conservative approach. We study this expectation and its effects on the DEL estimations in each case in the following sections.

195 2.4 Resistance and damage models

Material fatigue resistance tests are often performed under constant-amplitude cyclic loading. The information regards the number of cycles in each stress amplitude level that a test specimen can endure before failing is collected within S-N curves. Basquin formulation (Basquin, 1910) is a linear regression of the $\log N - \log S$ data points valid for most materials in the



region between approximately $1e3$ and $1e6$ cycles, where a linear fatigue behavior of the material in a log-log plot is expected.
200 Equation 7 shows the Basquin relationship.

$$N = kS^m \quad (7)$$

In Eq. (7), N is the number of endured (allowed) cycles in the stress amplitude equal to S . Both m (the fatigue exponent, also known as Wöhler's exponent) and k (the Basquin coefficient) in Eq. (7) are material specific. The Basquin regression model contains uncertainty. In addition, there is also physical and measurement uncertainty included in the material properties
205 and the tests. In the Basquin representation, m and K reflect the same sources of uncertainty as they are strongly correlated (an increase of one decreases the other in the regression). Thus, it is enough to model only one of them as the random variable to describe the scatter of the fatigue strength test data (Kececioglu, 2002; Veers, 1996). Following the common approach, we only consider the variability in the k parameter in the $\log N - \log S$ curve and assume Wöhler's exponent to be deterministic. Following available data regards average values of m , we assume the constant fatigue exponent to be equal to 10 in the case
210 of the composite and equal to 3 in the case of steel components. Thus, since we study the blade's flapwise and the tower base fore-aft load channels, we consider two different cases of $m = 10$ and $m = 3$ corresponding to the blade and the tower, respectively. We consider both compression-compression and tension-tension fatigue data for the fatigue analysis in the case of the flapwise bending moments according to (Mikkelsen, 2020) and the resulting time series of the current study.

In the case of variable loadings, such as in wind turbines, one should use a suitable model to relate the constant amplitude
215 data to the accumulated damage. Palmgren–Miner (Miner's) rule (Palmgren, 1924; Miner, 1945) is a common linear model with the same application. Equation 8 presents Miner's rule.

$$D = \sum_{i=1}^{N_s} \frac{n_i}{N_i} \quad (8)$$

In Eq. (8), parameter D accounts for the magnitude of fatigue damage, n_i is the number of cycles of the i th load amplitude
220 in the loading, and N_i is the allowed number of cycles according to the S-N curve of the material. In addition, N_s accounts for the total number of stress amplitude levels. According to Miner's rule, failure happens when the summation in Eq. (8) is higher than the material limit, often assumed equal to unity.

The blade's root cross-section in the case study wind turbine is nearly circular and we assume it to be circular in the current
225 study. In both cross-sections of the blade root and the tower base, Eq. (9) can represent the relation between the moments and stresses.

$$S_i = \frac{Mx_i c}{I_y} \quad (9)$$

In Eq. (9), Mx_i is the moment corresponding to the stress level S_i . In the current study, the direction y corresponds to the global direction of the wind in the HAWC2 simulations since we are considering the root in the blade, and the local coordinate



system of the tower base section is also aligned with the global coordinate system. Thus, we consider moments in the perpen-
 230 dicular direction (M_x). In addition, the section parameters c and I_y are the radius and the moment of inertia in the direction
 perpendicular to the moment's direction, respectively. Table 2 presents the values for c and I_y parameters in the blade's root
 and tower base cross-sections in the structural model of DTU 10MW reference wind turbine.

Table 2. Blade root and tower base section parameters of the DTU 10MW model in HAWC2

Cross section	radius (m)	In-plane moment of inertia (m^4)
Blade's root	1.765	4.837
Tower base	4.15	8.416

Using Eq. (7) and replacing the stresses with the corresponding load/moment amplitudes, Eq. (8), can be rewritten as Eq.
 235 (10).

$$D = \left(\frac{c}{I_y}\right)^m \sum_{i=1}^{N_s} \frac{n_i M_i^m}{k} \quad (10)$$

The parameter M_i in Eq. (10) represents the load/moment ranges in the time series. We use Eq. (10) to estimate the damage
 equivalent load (DEL), a parameter that we use in the current study to represent damage. The following section describes DEL.

2.4.1 Damage equivalent load

240 Damage-equivalent load (DEL) is a tool to compare the damage that two different loading scenarios with variable amplitude can
 cause. Burton et al. (2011) defines DEL as the magnitude of the constant-amplitude load or stress causing the same damage as
 the variable amplitude loading with the same equivalent number of cycles (N_{eq}) causes. Equation (11) shows the mathematical
 expression of this definition based on Miner's rule (Eq. (10)).

$$\frac{N_{eq}(E[DEL_s^m])}{k} \left(\frac{c}{I}\right)^m = \frac{\sum_{i=1}^{N_s} (n_i M_i^m)}{k \left(\frac{c}{I}\right)^m} \quad (11)$$

245 In the above Eq. (11), DEL_s is the DEL of a sample of 10-minute time series containing N_s number of stress bins and N_{eq}
 is the reference number of cycles. In the current study, we set N_{eq} equal to 951 cycles corresponding to the average number
 of cycles in a 10-minute interval based on the simulations of DTU 10MW turbine with DLC 1.2 load case conditions. Both
 sides of Eq. (11) represent the expectation of damage in a time span of 10 minutes. We use the expression on the right side
 to simplify the reliability assessment procedure and to be able to separate the variability of the load from material properties.
 250 We use Eq. (12) and Eq. (13) to calculate the lifetime damage estimation ($DEL_{lifetime}$) from the 10-minute sample DEL
 estimations.



$$E[(DEL_{bin})^m] = \sum_{s=1}^{SS} \frac{(DEL_s)^m}{SS} \quad (12)$$

In Eq. (12), SS is the number of 10-minute samples with the same mean wind speed and turbulence (same wind condition) but with different wind realizations (different turbulence seeds). Furthermore, DEL_{bin} is the DEL estimation in each wind condition (wind bin). In all current study cases, SS is equal to 200 (see Table 1).

$$E[DEL_{lifetime}^m] = \sum_{bin} E[(DEL_{bin})^m]P(bin) \quad (13)$$

In Eq. (13), $P(bin)$ corresponds to the joint probability of each wind condition (wind speed and turbulence). Since we are considering the marginal probability of turbulence conditioned on the mean wind speed bin, the joint probability is equal to the multiplication of the two marginal probabilities. Thus, Eq. (14) is another representation of Eq. (13).

$$E[DEL_{lifetime}^m] = \sum_{V_{bin}=v_L}^{v_U} \sum_{T_{bin}=t_L}^{t_U} E[(DEL_{bin})^m]P(T_{bin}|V_{bin})P(V_{bin}) \quad (14)$$

In Eq. (14), the variables T_{bin} and V_{bin} represent the mean wind speed and turbulence in each wind bin and $P(V_{bin})$ is the probability of occurrence of each mean wind speed (see Eq. (1)). In addition, the parameters v_L and v_U as well as t_L and t_U represent the lower bound and higher bound for mean wind speed and turbulence in each wind bin. Furthermore, $P(T_{bin}|V_{bin})$ is the conditional probability of each turbulence in each mean wind speed bin.

In study case 1 (constant turbulence), the probability of the representative value of turbulence is assumed to be equal to 1. The following section presents the mathematical relations and procedures for estimation of the fatigue reliability.

2.4.2 Fatigue reliability assessment

Structural reliability is the ability of a structure to fulfill the structural design request for a defined period of time (ISO 2394, 2015). Equation (15) shows the probabilistic representation of this ability as a function of time.

$$R(t) = 1 - P_f(t) \quad (15)$$

In Eq. (15), $P_f(t)$ is the probability of failure at time t and can be stated as the probability of exceeding a certain level. Commonly, this problem is referred to with a function named limit state function ($g(x, t)$) and the safe region is where this function is positive. In the design phase, the designer sets a level of reliability for the lifetime, which accounts for an optimal balance between failure consequences, cost of operation and maintenance, material costs, and the probability of failure



(Sørensen, 2015). In the present work, we perform the probabilistic reliability assessment by taking the following steps as described in (Madsen et al., 2006):

1. Modeling of limit state equation $g(X)$.
2. Quantification of uncertainties and modeling by stochastic variables X .
- 280 3. Applying reliability methods to estimate the probability of failure (first-order reliability method in the current cases)

The limit state function in the assessment of safety within at time t can be written as Eq. (16).

$$g(X, t) = R(X, t) - S(X, t) \quad (16)$$

In Eq. (16), R indicates the resistance of the component and S is the loading. In addition, X represents a set of stochastic variables whose uncertainty propagates through the load and resistance. In the present study, we assess the reliability in time intervals equal to 1 year and the time would remain constant through each reliability assessment. Thus, in the continuing, we eliminate t from the relations and notations to simplify. Failure occurs if the function g in Eq. (16) is smaller than or equal to zero. In other words, the probability of failure is the probability of the limit state function being equal to or less than zero. Accordingly, the probability of failure can be defined as Eq. (17).

$$P_f = \int \mathbb{1}_{g(x) < 0} f_x(X) \quad (17)$$

290 Miner's rule does not consider the load sequence effect in variable loading and thus leads to errors in the prediction of fatigue damage. There are some studies (Schaff and Davidson, 1997; Yanan et al., 1991; Rognin et al., 2009) showing high errors in the fatigue estimation of the composite materials, often in the form of overestimation, when using Miner's rule. We account for the uncertainty in Miner's rule by defining the limit of damage as a random variable with a mean value of 1 (Miner's rule limit for failure). With such an assumption, the limit state function for fatigue failure can be specified as Eq. (18) marquez2012fatigue.

$$295 \quad g(X) = \Delta - D \quad (18)$$

In Eq. (18), Δ represents the fatigue limit in Miner's rule as a random variable with a mean value equal to unity. Using Eq. (11) for defining the damage, Eq. (18) can be rewritten as Eq. (19).

$$g(X) = \Delta - \frac{NeqDEL_{lifetime}^m}{k} \left(\frac{c}{I}\right)^m \quad (19)$$

The limit state function in a specific time can be shown via different expressions other than the common form in Eq. (18). Equation (20) presents one of such alternatives (Dimitrov, 2013). In the present work, we use Eq. (20) since it facilitates the separation of the fatigue loads from the material properties as well as the use of simple fatigue reliability estimation methods because of linearization.



$$G(X) = \log\left(\frac{R(X)}{S(X)}\right) \quad (20)$$

Combining Eq. (19) and (20), the limit state function in the current study would be as Eq. (21).

$$305 \quad G(X) = \log(\Delta) - \log(Neq) - m\log\left(\frac{c}{I}\right) + \log(k) - m\log(DEL_{lifetime}) \quad (21)$$

The parameters $\log(Neq)$ and $m\log\left(\frac{c}{I}\right)$ in Eq. (20) are constants. Thus, the above equation consists of three random parameters related to the linear damage accumulation model ($\log(\Delta)$), material Resistance ($\log(k)$), and load ($\log(DEL_{lifetime})$).

In other to find the probability of failure, after defining the limit state function, the integration in Eq. (17) must be solved. This integration is hard to solve analytically and thus, there are established methods for estimating the answer. Some of the
310 commonly used methods are the first-order or second-order reliability methods or Monte Carlo (MC) simulations (see (Melchers and Beck, 2018) for further details about each method). Veers (1990) shows that the probability of failure of a wind turbine blade joint with a target life of 20 years can vary from 2.2% when using the second-order reliability method (SORM) to 1.8% when using the first-order reliability method (FORM). However, since we have simplified the formulation of the limit state function to a linear summation of the random variables, we expect the first-order reliability method to be suitable for solving
315 the problem and we validated it by comparing the results of one of the case scenarios using FORM and MC. Thus, we use the FORM in the current work for both reliability assessment and defining the importance of the inputs. The next section contains more details about this method.

2.4.3 FORM and importance ranks

320 As stated in the previous subsection, the FORM is one of the ways to estimate the solution of the integration in Eq. (17). In this method, the problem of the limit state function being more or less than zero is redefined in the Standard Normal space. In other words, all the distributions of the random variables are transformed to Standard Normal distribution, and the expression of the limit state function is also transformed. In Standard Normal space, the probability of failure problem will change into looking for an optimum design point (X^* or correspondingly U^* in the standard normal space) that lies on the curve of $g(U) = 0$
325 and has the minimum distance from the origin. The corresponding distance is known as the reliability index (β). The reliability index is commonly used as a measure of structural reliability (for more details about FORM see (Melchers and Beck, 2018)).

Equation (22) shows the relationship between the reliability index and the probability of failure (Gulvanessian et al., 2012).

$$\beta = -\Phi^{-1}(P_f) \quad (22)$$

330 The operator Φ^{-1} shown in Eq. (22) corresponds to the inverse cumulative distribution function (CDF) of the standard normal distribution.



The ISO standard (ISO 2394 (2015)) presents the basic recommendation concerning a required reliability level in terms of the reliability index related to a certain reference time. The minimum required reliability index is known as target reliability. Based on (IEC 61400-1, 2005), a target value for the nominal failure probability for structural design for fatigue failure mode of the wind turbine components in a reference period of 1 year is $5e - 4$ corresponding to a target reliability of 3.3 according to Eq. (22). More specifically, Veldkamp (2007) performed a cost-benefit analysis and reported the optimal reliability level for the blade to be 2.7 (probability of failure of $3.5e - 3$) based on the analysis. In the present work, we study the sensitivity of reliability to different variables and not the levels. However, we present the reliability levels in different cases of the study as well. We consider $R = 10$ for fatigue properties of the composite (Mikkelsen, 2020).

In order to apply FORM analysis, first, we fit distributions to the estimations of $\log(DEL_{lifetime})$ calculated based on 10-minute simulations using Eq. (14). It is more realistic to assume that different materials will have a different range of Δ because of differences in the scatter of the strength data which will in turn result in different distribution parameters (Le and Peterson, 1999). We gather and re-use the information about the distributions and statistical parameters of the material and Miner's rule limit from the literature. Since the DTU 10-MW turbine is not designed against fatigue, we observed low-reliability levels in the blade root and the tower base (failure occurrence in the tower base). Thus, in the current study, we increase the material fatigue strength proportional to the high fatigue loads while keeping the corresponding coefficient of variation (CoV) the same as real material to avoid effects on the sensitivity analysis. These changes will affect our reliability levels. However, the main interest in the current study is the sensitivities and changes, not the values. Table 3 shows this information plus the references for the coefficients of variation.

350

Table 3. Characteristics of the material and model variables

Variable	Component	Distribution	mean	std	Reference
$\log(\Delta)$	blade	Normal	-0.1116	0.4724	(Toft and Sørensen, 2011; Stensgaard et al., 2016b)
	tower	Normal	-0.0431	0.2936	(Stensgaard et al., 2016b)
$\log(K)$	blade	Normal	calibrated	0.602	(Mortensen et al., 2023; Toft and Sørensen, 2011)
	tower	Normal	calibrated	0.2	(Sørensen, 2015; Slot et al., 2019)

After specifying all the distributions and probabilistic parameters of each random variable in Eq. (21), we transform each non-Normal distribution to Normal using the Normal-tail approximation and Rackwitz-Fiessler algorithm (Rackwitz and Fiessler, 1978) to find the optimum design point. The following contains the relations and procedures for the transformation and solving procedures.

In transforming of non-Normal continuous distributions to Normal, since the design points (X^*) are usually located at the tail of the corresponding Normal distribution, we estimate the corresponding mean $\mu_{x_i^*}$ and standard deviation $\sigma_{x_i^*}$ based on the design point x_i^* using Eq. (23) and Eq. (24), respectively (Rackwitz, 2007).



$$\sigma_{x_i^*} = \frac{\phi(u_i^*)}{f(x_i^*)} \quad (23)$$

$$\mu_{x_i^*} = x_i^* - \sigma_{x_i^*} u_i^* \quad (24)$$

360 In Eq. (23) and Eq. (24), the operator ϕ is the cumulative distribution function (CDF) of standard Normal distribution and f corresponds to the PDF of the initial non-Normal distribution. In addition, x_i^* is the non-normally distributed random variable in the design point (X^*) and u_i^* is the corresponding element in the design point in the standard normal space (U^*). u_i^* is acquired as Eq. (25).

$$u_i^* = \Phi^{-1}(F(x_i^*)) \quad (25)$$

365 F in Eq. (25) stands for the CDF of the point in the initial distribution. In fact, Eq. (25) presents the basic concept that in the transformation process between different distributions, the probability of each point remains unvaried.

This method also provides information regards the importance level of each random variable or in other words, the sensitivity of the output to each input. A vector α provides such information. Eq. (26) and Eq. (27) show the expressions for this vector and the importance factor of each parameter based upon.

$$370 \quad \alpha = -\frac{\nabla g(u^*)}{|\nabla g(u^*)|} = \frac{u^*}{\beta} \quad (26)$$

$$Importance\ factor = \frac{\alpha_i}{|\alpha|} \quad (27)$$

Since α is a unit vector, the denominator in Eq. (27) is equal to one, and thus, α_i is the importance factor for variable x_i . Eq. (28) and Eq. (29) present the formulation for calculating the annual probability of failure and an annual reliability index (Velarde et al., 2019).

$$375 \quad \Delta P_f(X, t) = \frac{P_f(X, t + \Delta t) - P_f(X, t)}{(1 - P_f(X, t)) \Delta t} \quad (28)$$

$$\Delta \beta(X, t) = -\Phi^{-1}(\Delta P_f(X, t)) \quad (29)$$

2.4.4 Sampling

380 To fit distributions to DEL data in different case studies, we need to sample from the turbulence distribution in each wind speed bin to account for turbulence probability (see Eq. (14)). For sampling turbulence levels from cases 2 and 3, we divide their corresponding probability space into 5% probability intervals and then we take the median of each probability interval as the representative. We derive the corresponding turbulence sampling point by taking the inverse of the CDF at the median point. Following such an approach, we can account for all probability levels equally. The probability of each sampling point is equal
 385 to 5%. Fig. 3 shows the resulting sampling points in different mean wind speeds.

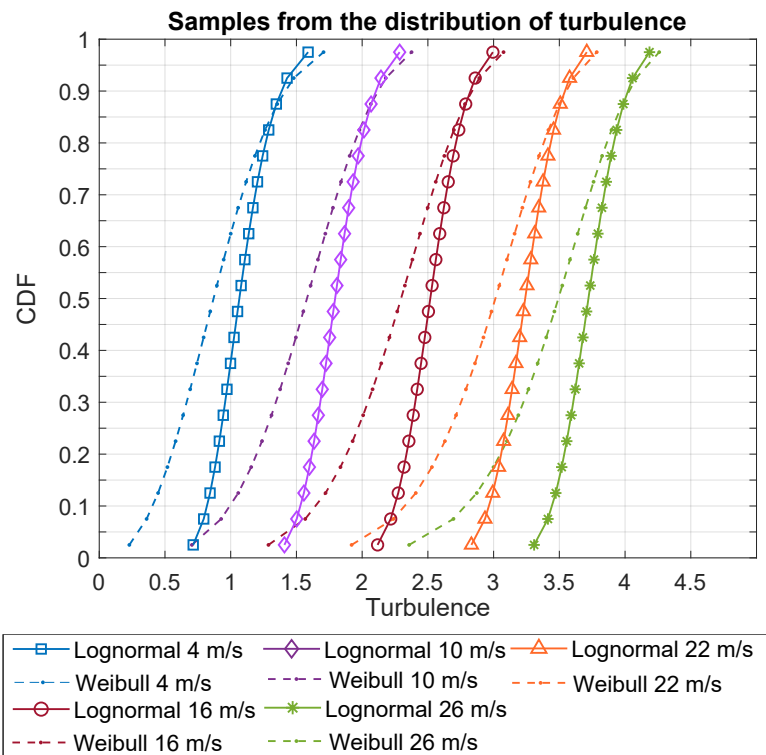


Figure 3. Sampling points of turbulence within intervals of size 0.05 in the corresponding in case 2 (lognormal distribution) and case 3 (Weibull distribution)

Fig. 3 reveals that the turbulence levels within the same probability are higher in case 2 (lognormal distribution) compared to case 3 (Weibull distribution). The differences are higher in the higher turbulence levels with lower probability, especially, in higher mean wind speeds.

The following section provides the results of the study.



390 3 Results and discussions

The current section presents the results of the study in two steps. First, we introduce the distributions of DEL in different turbulence modeling cases in Sect. 3.1. Then, we investigate the change of fatigue reliability through time in different turbulence models and in different Wöhler curve exponents in Sect. 3.2. Sect. 3.3 contains the sensitivity analysis of the reliability of each input in different scenarios. Finally, Sect. 3.4 includes supplementary discussions about the results. All the results are provided
395 for both the blade root flapwise and tower base fore-aft load channels.

3.1 Probability distributions and statistical parameters of load

Wind fluctuation is one of the main causes of fatigue damage, especially in the load channels like the blade flapwise and tower fore-aft. Thus, if we set the mean stress level constant, the higher load fluctuations (higher standard deviation in the loads) cause higher fatigue damage in the components. Therefore, a change in the wind standard deviation (turbulence) in each mean
400 wind speed level directly changes the estimated fatigue damage. In the current section, we look into the change in the distribution of DEL with the change in turbulence characterization method in the IEC Normal Turbulence Model. In case 1, each realization of DEL_{bin} is based on one turbulence level (representative turbulence) while in the other two cases (considering lognormal and Weibull distributions for turbulence), each realization is a result of integration over all 20 turbulence levels each represented via one realization.

405

Fig. 4 shows DEL_{bin} values resulting from different turbulence levels and seeds using (Eq. 12) in cases 2 and 3. Fig. 4 only contains the fatigue exponent considered in the design, which is equal to 10 in the blade root and equal to 3 in the tower base.

The bar plots of Fig. 4 show the binning over mean wind speeds and turbulence levels we sample with equal probability over the domain. It reveals the increase of the DEL with an increase in mean wind speed and standard deviation of the wind.
410 The only exception to this trend is the DEL in the tower base around mean wind speeds of 6 m/s and 8 m/s. The reason is that around these mean wind speeds, there is a local peak in DEL values because of the resonance (Mozafari et al., 2023).

Another observation from Fig. 4 is the relatively faster decrease of the tower-base DEL_{bin} as a function of turbulence compared to the blade. This observation reveals that the variability in the case of the tower base is much higher in each wind bin (check (Mozafari et al., 2023) for more details). Thus, we expect the integration over all turbulence levels (see Eq. (14)) to
415 be more effective in decreasing variability in tower base DEL_{bin} and thus, $DEL_{lifetime}$ estimations. The following includes observations on $DEL_{lifetime}$ distributions.

Using the 200 samples in each wind bin (consisting of constant turbulence and constant mean wind speed), we calculate the $DEL_{lifetime}$ using Eq. (13) in case 1 (constant 90% turbulence) and Eq. (14) in cases 2 and 3 (lognormal and Weibull
420 distribution). We take samples of size 6 from this database 1000 times with replacement (bootstrapping) to obtain the distributions of DEL when following IEC recommendations regarding the number of sample sizes. This method results in 1000 $DEL_{lifetime}$ realizations in each case. Fig. 5 shows the probability density function (PDF) of the $DEL_{lifetime}$ estimations in

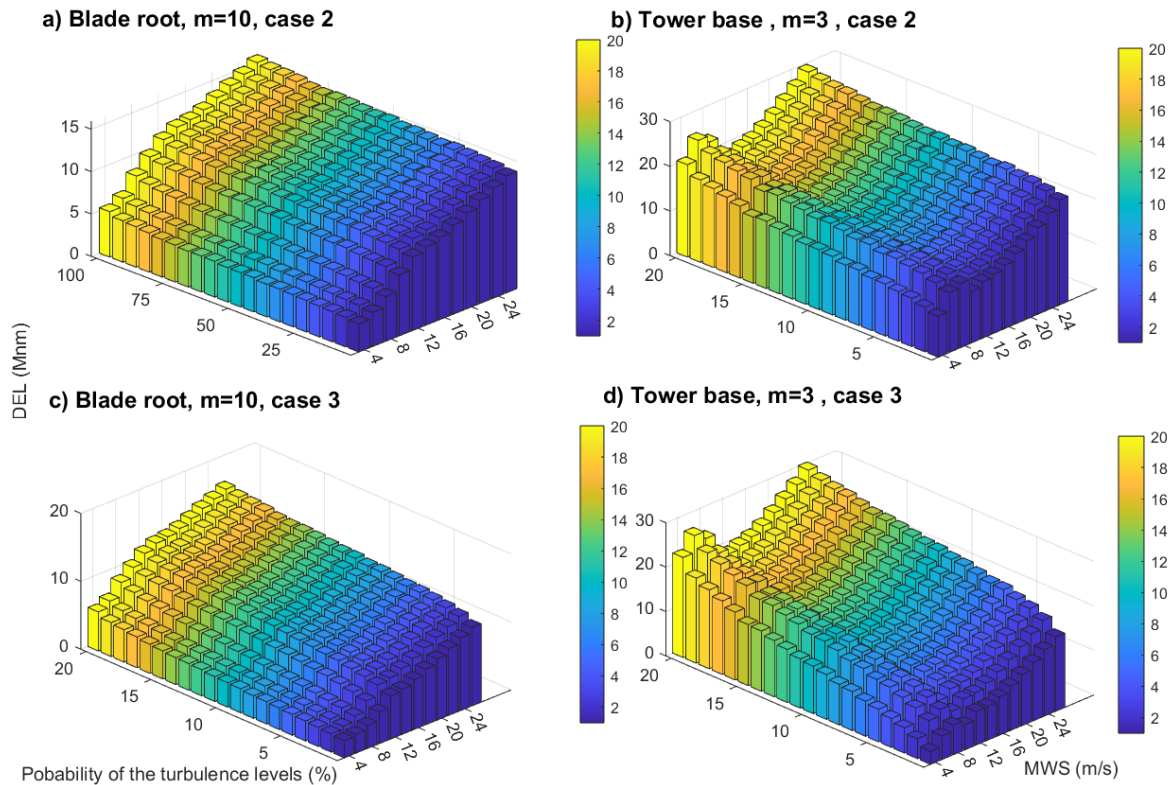


Figure 4. $DEL_{bin,s}$ in each mean wind speed and turbulence level in a) case 2 (Turbulence sampling based on lognormal distribution) for blade root b) case 2 for the tower base c) case 3 (Turbulence sampling based on Weibull distribution) for blade and d) case 3 for tower base (The results are only shown for comparison and the DEL dimensions are relative)

different turbulence cases and different fatigue exponents in both load channels under study. The results are all normalized by the mean of the Case 1 data in each condition.

425 Fig. 5 reveals that the overall variability of the $DEL_{lifetime}$ realizations are higher in the case of the tower base compared to the blade root, as expected due to the reasons discussed above and in (Mozafari et al., 2023). This remains the case for all methods of turbulence modeling. The distributions are not significantly impacted by the fatigue exponent, as indicated by the similarity of the distributions in the different rows.

430 Based on Fig. 5, the integration over turbulence distributions (cases 2 and 3) instead of using one representative value (case 1) not only decreases the mean value but also the variance of the realizations. This effect is more notable in the case of the tower base. This is expected, as 4 shows that the variability in the tower base DEL_{bin} is larger than in the blade-root moment. The lower variance of the $DEL_{lifetime}$ realizations is partly because in the calculations of this parameter in cases 2 and 3 we do one extra step of integration. The other reason is considering lower turbulence levels instead of focusing on the upper tail

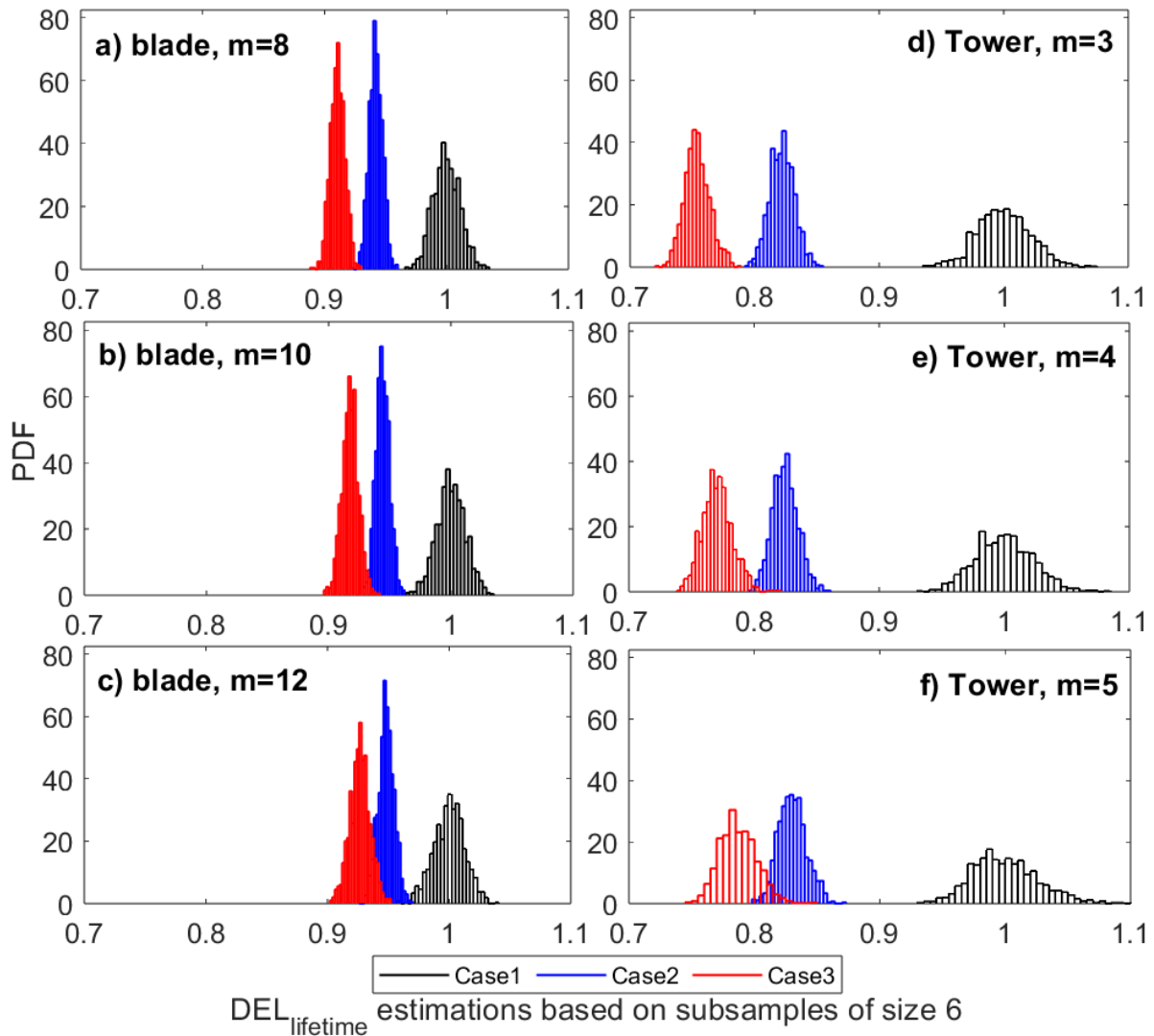


Figure 5. PDF and the best distribution fits to DEL estimates using 1000 bootstrap samples of size 6 in different turbulence study cases based on a) blade root flapwise, $m = 8$ b) blade root flapwise, $m = 10$ c) blade root flapwise, $m = 12$ e) tower base fore-aft $m = 3$, f) tower base fore-aft $m = 4$, g) tower base fore-aft $m = 5$

435 of the distribution (90% quantile in this case).

Comparing the distributions of $DEL_{lifetime}$ in case 2 (lognormal) and case 3 (Weibull) in Fig. 5 reveals that the mean levels in case 2 are lower than in case 3. In other words, the estimation of $DEL_{lifetime}$ based on the Weibull distribution of turbulence is less conservative compared to the lognormal distribution approach. This complies well with the expectations based on the characteristics of the two distributions discussed in Sect. 2.4.4. The bias in the mean value of $DEL_{lifetime}$ calculated with the

440



Weibull/lognormal distributions is more significant for the tower base than the blade root; thus, using representative turbulence is much more conservative in the case of the tower base. For example, in the case of the tower with a fatigue exponent of 3, the $DEL_{lifetime}$ estimation can vary by more than 35% when using 6 seeds.

445 There is an overlap between distributions of all cases in the blade root and between cases 2 and 3 in the tower base. This means if the designer uses only 6 realizations, there is a chance that the $DEL_{lifetime}$ estimation using Weibull distribution is more conservative than the lognormal. For example in the tower base with a fatigue exponent of 5, $DEL_{lifetime}$ estimations in case 3 can be around 5-7% more conservative than case 2. In addition, in the blade root, when using 6 seeds, lognormal can provide a less conservative DEL estimation than the 90% turbulence level model. Although such occurrences are very rare, the
 450 chances increase with an increase in the fatigue exponent in each load channel.

The general conservatism of using a 90% turbulence level in the DEL evaluations can show itself in the fatigue reliability estimations. In addition, since changing the method of modeling the turbulence changes both the mean and standard deviation of the DEL realizations, the sensitivity of the reliability levels to the DEL can also differ from one case to another. We study the
 455 extent of such effect and the change in that with the change in fatigue exponent in the two load channels in the next subsections.

3.2 Fatigue reliability in different cases

In the reliability assessments, we use the $\log(DEL_{lifetime})$ as the parameter representing the load (see Eq. (21)). To complete the reliability analysis, we need to determine an appropriate probability distribution for the load parameter. Thus, we first find the probability distributions of $\log(DEL_{lifetime})$ in different conditions (each condition includes a load channel, a
 460 turbulence modeling case, and a specific fatigue exponent). Tables 4 and 5 represent some of the best distribution fits to the $\log(DEL_{lifetime})$ data and their parameters in three different turbulence model cases in $m = 10$ and $m = 3$ for the blade root and tower base, respectively (for more cases see appendix).

Table 4. Best distribution fits to $\log(DEL_{lifetime})$ in different turbulence modeling cases considering flapwise bending moments in the blade root ($m = 10$)

Case	Distribution	Par 1	par2	par3
1 (Representative turbulence)	GEV	-0.299	0.012	2.405
2 (lognormal turbulence)	GEV	-0.239	0.006	2.349
3 (Weibull turbulence)	Normal	2.323	0.007	-

Using the distributions of $\log(DEL_{lifetime})$ and the distributions of other parameters ($\log(\Delta)$ and $\log(K)$) as we previously defined in Table 3, we estimate the annual reliability and its change through the lifetime (see Eq. (29) and Eq. (28)). It should
 465 be noted that although we derive different distributions of $\log(DEL_{lifetime})$ in the case of different Wöhler exponents, the distributions in 3 are only referring to the reference levels of this exponent in the design. Thus, for the sake of comparison

Table 5. Best distribution fits to $\text{Log}(DEL_{lifetime})$ in different turbulence modeling cases considering fore-aft bending moments in the tower base ($m = 3$)

Case	Distribution	Par 1	par2	par 3
1 (Representative turbulence)	lognormal	1.11	0.01	-
2 (lognormal turbulence)	Normal	2.824	0.0118	-
3 (Weibull turbulence)	GEV	-0.22	0.01	2.73

of the trends, we modify the mean value of $\log(K)$ in different variations of fatigue exponents ($m = 4, m = 5$ for the tower and $m = 8, m = 12$ for the blade) in a way that we get the same reliability level in the first year. Fig. 6 shows the change of reliability over 20 years in the blade root and the tower base in different conditions.

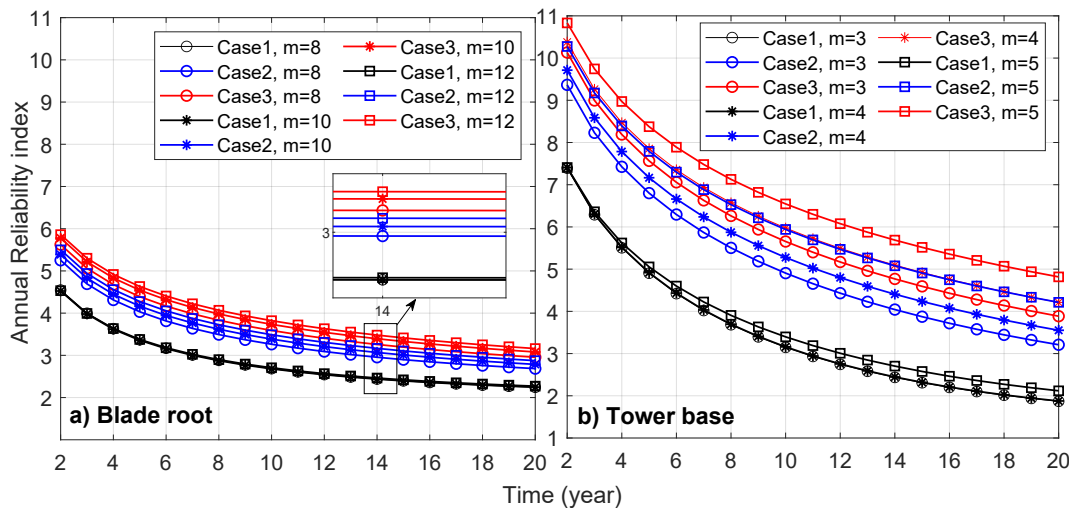


Figure 6. Reliability index through the lifetime in a) blade's flapwise and b) tower base fore-aft load channels in cases 1, 2, and 3 considering different Wöhler exponents

470 The results in Fig. 6 show that the in both load channels and different fatigue exponents, constant turbulence (black lines) provides conservative results in terms of annual reliability level. The next conservative evaluation belongs to lognormal (blue lines) and the last to Weibull (red lines). The ranks remain the same in all cases. In other words, the overlaps in the distributions of DEL observed in Fig. 5 between cases 2 and 3 are not seen in Fig. 6 and do not affect the reliability. We explain the reason in the sensitivity analysis presented in the next section.

475

In general, the tower base shows a very fast reduction in reliability over time. One possible reason is the higher mean value of the $\log(DEL_{lifetime})$ especially verses material fatigue resistance ($\log(K)$) in this load channel. We are using the conventional method of linear scaling the damage with time. In a high DEL magnitude, this method leads to a fast increase in damage



over time.

480

In the case of constant turbulence in the tower base, the change in the fatigue exponent ('m') has a more visible effect on the rate of reliability declination through time. In this case, a larger in 'm' increases the decline in reliability level from the same initial point at year 2.

485

Notice that the results seen in the tower base are more visible because of the higher initial variability in the DEL in this load channel. In the case of the blade, the same trends occur but they are less visible.

3.3 Importance ranks of the inputs

We study the sensitivity of the reliability level at 20 years to each of the random inputs in the limit state function. The importance rank of each of the inputs is derived based on FORM analysis (see Eq. (27)). The relative importance levels in different cases and fatigue exponents are shown in Fig. 7 and Fig. 8 for the blade root and tower base, respectively. It should be noted that in these plots, the extent of differences is not representative of the absolute importance of the load, material fatigue strength, and Miner's rule we model the logarithm of each of the variables, and the levels of magnitude are very different. However, they show relative importance in terms of rank. In addition, the change in the percentages from one case scenario to another is still a good measure for comparing sources of uncertainty and tracking changes in the sensitivities.

495

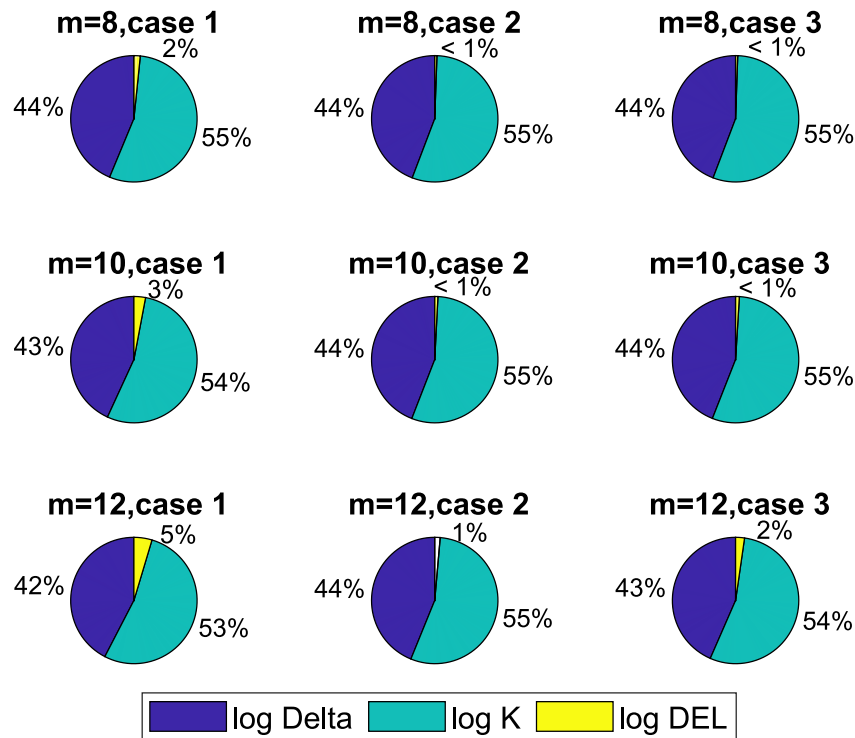


Figure 7. Importance factors of different random inputs in assessing annual reliability level at year 20 in blade’s flapwise load channel in cases 1, 2, and 3 considering different Wöhler exponents

Fig. 7 shows the relatively high importance of the fatigue resistance of the material in the blade root. The second important parameter is the uncertainty in the fatigue accumulation model. Their relative effects are much higher than the loads because of the low variance of load in the blade. The lower variance in the DEL when using integration over turbulence in each wind speed bin (as shown before in Fig. 5) decreases the effect of this parameter on the reliability level. The share of the load in the overall reliability increases with the increase of fatigue exponent as we expect. However, the importance of the load uncertainty compared to the other two parameters is negligible.

Fig. 8 shows the relatively high importance of the miner’s rule uncertainty as the coefficient of variation in $\log(K)$ in steel (material in the tower base) is much lower than in the composite (in the blade). The second effective parameter is the fatigue resistance of the material and the load is the least important part of the uncertainty in the reliability.

The effects of the fatigue loads on the reliability in the tower base are relatively higher than in the case of the blade root (see Fig. 7). This is because of the higher CoV in the fatigue loads in the tower base.

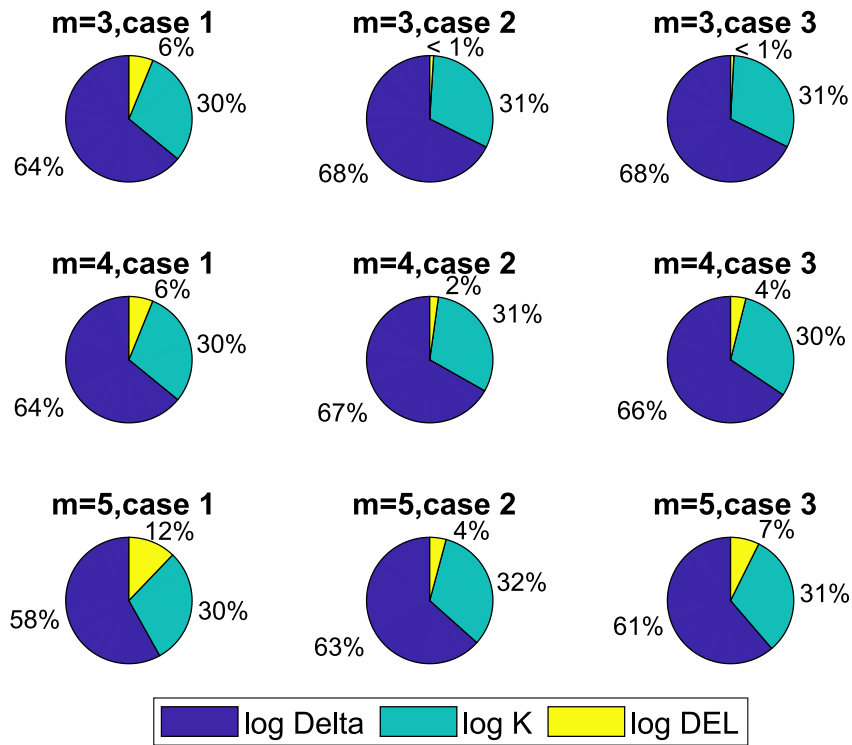


Figure 8. Importance factors of different random inputs in assessing annual reliability level at year 20 in tower base fore-aft load channel in cases 1, 2, and 3 considering different Wöhler exponents

As seen in the previous load channel (blade root flapwise), we observe an increase in the importance of the loads with an increase in the fatigue exponent. In addition, the case 2 and 3 turbulence modeling decrease the CoV of $\log(DEL)$ and thus its importance in fatigue reliability.

According to both Fig. 7 and Fig. 8, there is no obvious change in the importance factors when changing the distribution from lognormal to Weibull. In other words, the change in CoV of DEL is very low when changing the distribution of turbulence.

515 3.4 Overall discussions

The results (especially in Fig. 6) reveal the high importance of the fatigue exponent in the tower base in design-level reliability estimations. The fatigue strength curves of the steel structures are normally bi-linear and the selection of the fatigue exponent at the design level especially when using equivalent forms like DEL can vary between the lower, the higher, or the average slope. The results in the current work elaborate on the importance of focusing on the characterization of the steel fatigue exponent at the design level as the annual reliability levels of the tower base (normally experiencing high loads) are very sensitive to this



parameter.

The results of reliability estimations show that the small overlaps seen in the DEL distributions are not very important when coming into the reliability framework. This has been made more clear in the sensitivity analysis.

525

A potential concern with the results is the difference in sample size for the different cases. In particular, there are more 10-minute simulations involved in estimations in cases 2 and 3. A larger sample size naturally decreases the variance in the $DEL_{lifetime}$ evaluations due to the law of large numbers (see (Mozafari et al., 2023) for more details). To investigate whether this is significant, we checked the effect by using different combinations of seed numbers and the corresponding effect on the trends is negligible.

530

Since the distributions in the IEC standard NTM are functions of parameters for each class of wind turbine (see Eq. (2) to Eq. (6)), the results depend on the class. We re-performed the study for a lower reference turbulence intensity more suitable for offshore cases (0.1) and the trends were the same in terms of DEL distribution biases. However, we encourage similar studies on different classes of wind turbines to track the possible differences in terms of magnitudes.

535

All in all, although the choice of the turbulence characterization approach impacts the reliability and the sensitivity of the reliability to different uncertainty sources, these effects are not notable when compared to the high sensitivity of the reliability to other sources in every case. In other words, accurate modeling of the damage accumulation or more accurate characterization of the material properties (especially in the case of composites) can impact the reliability levels to a much higher extent. Considering the 50% change in the reliability level at year 20 in the case of the tower base with $m = 5$, and the fact that the uncertainty in the material properties, in this case has around 8 times higher impact than load, the changes can be drastic.

540

There are also some limitations to consider when using the results of the current study. For example, the thickness of the tail in the lognormal distribution is dependent on its standard deviation which in different cases of NTM, is a function of the reference turbulence level in each mean wind speed. This means that there is a possibility that the results of the current study change with the wind turbine class. Therefore it is valuable to investigate the case of lower reference turbulence levels to come to general conclusions.

545

In addition, doing the same reliability analysis using Monte Carlo instead of FORM can provide more accurate reliability estimates in the case of having computational resources.

550 4 Conclusions

The assessment of the remaining fatigue lifetime hinges upon the re-analysis of the reliability. In performing such an analysis per the IEC standards, a designer can choose to follow different recommendations in the IEC standards regarding characterizing turbulence, but the ramifications of those choices are currently unclear. For example, as shown by the current study, using 6



realizations for the estimation of DEL, in the case of the tower with a fatigue exponent of 3, the DEL estimation based on case
555 3 (the Weibull distribution of turbulence) can differ by 40% from the representative turbulence case. In addition, the annual
reliability index after 20 years can differ by a factor of two (with Weibull distribution being less conservative). In terms of
fatigue reliability at the end of the design lifetime (20 years), the differences are up to 50% in the case of the blade root and
up to 200% in the case of the tower base. This high difference can change the possible scenarios at the lifetime extension stage
and must be taken into consideration.

560 The results presented in this paper are very applicable to the wind turbine design stage as they provide the designer with
information about the extent to which following different editions of the IEC standard can change the expected value and
uncertainty of the fatigue damage evaluations based on turbulence input. It also shows how the annual fatigue reliability and
sensitivity of reliability change in load channels of interest and different fatigue exponents.

565 The sensitivity analysis of the reliability reveals that although the change in the turbulence characterization changes the
distribution of the fatigue loads and the fatigue reliability, it is more effective to focus on decreasing the material or models'
uncertainty to have a more robust fatigue reliability assessment. This is because the overall importance of the fatigue loads
compared to the high uncertainties in the material properties and linear damage accumulation rule is negligible in both load
channels under study and different fatigue exponents. The change in the loads can vary. Furthermore, The reliability estimation
570 is based on a simplified linearized limit state function which makes the complete separation of the loads from material proper-
ties possible. In the case that all the random variables are lognormally distributed (which is highly possible), this formulation
results in a very simple and fast reliability analysis at the design level.

Using Monte Carlo simulations, testing for other wind turbine classes and the use of other aeroelastic tools for the same
575 study are some suggestions for future studies.

Appendices

The parameters of the best-fitted distributions to $\log(DEL)$ in different load channels under study and different fatigue expo-
nents are shown in Tables A1-D1.

Table A1. Best distribution fits to $\text{Log}(DEL_{lifetime})$ in different turbulence modeling cases considering flapwise bending moments in the
blade root ($m = 8$)

Case number	Distribution	Par 1	par 2	par 3
1 (Representative turbulence)	lognormal	0.822	0.005	-
2 (lognormal turbulence)	lognormal	0.795	0.003	-
3 (Weibull turbulence)	lognormal	0.780	0.003	-



Table B1. Best distribution fits to $\text{Log}(DEL_{lifetime})$ in different turbulence modeling cases considering flapwise bending moments in the blade root ($m = 12$)

Case number	Distribution	Par 1	par 2	par 3
1 (Representative turbulence)	Normal	2.510	0.013	-
2 (lognormal turbulence)	Normal	2.457	0.007	-
3 (Weibull turbulence)	Normal	2.434	0.009	-

Table C1. Best distribution fits to $\text{Log}(DEL_{lifetime})$ in different turbulence modeling cases considering fore-aft bending moments in the tower base ($m = 4$)

Case number	Distribution	Par 1	par 2	par 3
1 (Representative turbulence)	lognormal	1.176	0.007	-
2 (lognormal turbulence)	GEV	-0.218	0.012	3.044
3 (Weibull turbulence)	GEV	-0.180	0.015	2.975

Table D1. Best distribution fits to $\text{Log}(DEL_{lifetime})$ in different turbulence modeling cases considering fore-aft bending moments in the tower base ($m = 5$)

Case number	Distribution	Par 1	par 2	par 3
1 (Representative turbulence)	GEV	-0.169	0.023	3.396
2 (lognormal turbulence)	GEV	-0.201	0.013	3.216
3 (Weibull turbulence)	GEV	-0.194	0.017	3.162

<https://doi.org/10.5194/wes-2023-47>
Preprint. Discussion started: 12 June 2023
© Author(s) 2023. CC BY 4.0 License.



Author contributions. SM, PV, and JR were responsible for the overall conceptualization of the study. SM wrote all the computer codes and performed all the data analysis. SM, PV, and KD were involved in the writing, and editing of the manuscript

Competing interests. At least one of the (co-)authors is a member of the editorial board of Wind Energy Science.



References

- Bacharoudis, K. C., Antoniou, A., and Lekou, D. J.: Measurement uncertainty of fatigue properties and its effect on the wind turbine blade reliability level, EWEA, November, pp. 17–20, 2015.
- 585 Bak, C., Zahle, F., Bitsche, R., Kim, T., Yde, A., Henriksen, L. C., and Natarajan, A., H. M. H.: Description of the DTU 10 MW Reference Wind Turbine, in: DTU Wind Energy Report-I-0092, July 2013.
- Basquin, O. H.: The Exponential Law of Endurance Tests, in: ASTM, p. 625, 1910.585
- Burton, T., Jenkins, N., Sharpe, D., and Bossanyi, E.: Wind energy handbook, John Wiley & Sons, <http://dx.doi.org/10.1002/9781119992714>, 2011.
- 590 Choi, S., Canfield, R. A., and Grandhi, R. V.: Reliability-Based Structural Design, Springer, <http://dx.doi.org/10.1007/978-1-84628-445-8>, 2007.
- Commission, G. I. E.: IEC 61400-1, Wind turbine generator systems – Part 1: Safety requirements, 3rd edition ed, Proceedings of the IEC, pp. 61 400–3, 2005.
- Commission, G. I. E.: IEC 61400-1, Wind turbine generator systems – Part 1: Safety requirements, 4th edition ed, Proceedings of the IEC, 590 pp. 61 400–4, 2019.
- 595 Dimitrov, N. K.: Structural reliability of wind turbine blades: Design methods and evaluation, Ph.D., Technical University of Denmark, 2013.
- Dimitrov, N. K., Natarajan, A., and Mann, J.: Effects of normal and extreme turbulence spectral parameters on wind turbine loads, Renewable Energy, 101, 1180–1193, <http://dx.doi.org/10.1016/j.renene.2016.10.001>, 2017.
- Dimitrov, N. K., Kelly, M. C., Vignaroli, A., and Berg, J.: From wind to loads: wind turbine site-specific load estimation with surrogate models trained on high-fidelity load databases, Wind Energy Sci., 3, 767–790, <http://dx.doi.org/10.5194/wes-3-767-2018>, 2018.
- 600 Emeis, S.: Current issues in wind energy meteorology, Meteorological Applications, 21, 803–819, 2014.
- Ernst, B. and Seume, J. R.: Investigation of site-specific wind field parameters and their effect on loads of offshore wind turbines, Energies, 5, 3835–3855, <http://dx.doi.org/10.1002/met.1472>, 2012.
- Gulvanessian, H. and Calgaro, J. and Holický, M.: Designer’s guide to EN 1990: eurocode: basis of structural design, Thomas Telford, 2002.
- 605 Hansen, K. S. and Larsen, G. C.: Characterising turbulence intensity for fatigue load analysis of wind turbines, Wind Engineering, 29, 600 319–329, <http://dx.doi.org/10.1260/030952405774857897>, 2005.
- Ishihara, T., Yamaguchi, A., and Sarwar, M. W.: A study of the normal turbulence model in IEC 61400-1, Wind Engineering, 36, 759–765, <http://dx.doi.org/10.1260/0309-524X.36.6.759>, 2012.
- ISO 2394, I.: General principles on reliability for structures, Zurich: ISO, 2015.
- 610 Kececioglu, D.: Reliability engineering handbook, vol. 1, DEStech Publications, Inc, 2002.
- Larsen, G. C.: Offshore fatigue design turbulence, Wind Energy An Int. J. for Progress and Applications in Wind Power Conversion Tech., 4, 107–120, <http://dx.doi.org/10.1002/we.49>, 2001.
- Larsen, T. J. and Hansen, A. M.: How 2 HAWC2, the user’s manual, target, 2, 2007.
- Le, X. and Peterson, M. L.: A method for fatigue-based reliability when the loading of a component is unknown, Int. J. of Fatigue, 21, 603–610, [http://dx.doi.org/10.1016/S0142-1123\(99\)00016-X](http://dx.doi.org/10.1016/S0142-1123(99)00016-X), 1999.
- 615 Madsen, H. O., Krenk, S., and Lind, N. C.: Methods of structural safety, Courier Corporation, 2006.
- Mann, J.: Wind field simulation, Probabilistic Eng. Mech., 13, 269–282, [https://doi.org/https://doi.org/10.1016/S0266-8920\(97\)00036-2](https://doi.org/https://doi.org/10.1016/S0266-8920(97)00036-2), 1998.



- Márquez-Domínguez, S. and Sørensen, J. D.: Fatigue reliability and calibration of fatigue design factors for offshore wind turbines, *Energies*, 620 5, 1816–1834, <http://dx.doi.org/10.3390/en5061816>, 2012.
- Melchers, R. E. and Beck, A. T.: Structural reliability analysis and prediction, John Wiley & Sons, <http://dx.doi.org/10.1002/9781119266105>, 2018.
- Mikkelsen, L. P.: The fatigue damage evolution in the load-carrying composite laminates of wind turbine blades, in: *Fatigue Life Prediction of Composites and Composite Structures*, pp. 569–603, Elsevier, <http://dx.doi.org/10.1016/B978-0-08-102575-8.00016-4>, 2020.
- 625 Miner, M. A.: Cumulative damage in fatigue, <http://dx.doi.org/10.1115/1.4009458>, 1945.
- Mortensen, U. A., Rasmussen, S., Mikkelsen, L. P., Fraisse, A., and Andersen, T. L.: The impact of the fiber volume fraction on the fatigue on performance of glass fiber composites, *Composites-Part A: Applied Science and Manufacturing*, <http://dx.doi.org/10.1016/j.compositesa.2023.107493>, 2023.
- Mozafari, S., Dykes, K., Rinker, J. M., and Veers, P. S.: Effects of finite sampling on fatigue damage estimation of wind turbine components: A statistical study, *Wind Eng.*, <http://dx.doi.org/10.1177/0309524X231163825>, 2023.
- 630 Murcia, j. P., Réthoré, P., Dimitrov, N. K., Natarajan, A., Sørensen, J. D., Graf, P., and Kim, T.: Uncertainty propagation through an aeroelastic wind turbine model using polynomial surrogates, *Renewable Energy*, 119, 910–922, <https://doi.org/https://doi.org/10.1016/j.renene.2017.07.070>, 2018.
- Øistad, I. S.: Analysis of the Turbulence Intensity at Skipheia Measurement Station, Master’s thesis, NTNU, 2015.
- 635 Palmgren, A.: Die lebensdauer von kugellagern, *Zeitschrift des Vereines Duetsher Ingenieure*, 68, 339, 1924.
- Rackwitz, R.: Aspects of structural reliability: in honor of R. Rackwitz, Herbert Utz Verlag, 2007.
- Rackwitz, R. and Fiessler, B.: Non-normal vectors in structural reliability, 1978.
- Ren, G., Liu, J., Wan, J., Li, F., Guo, Y., and Yu, D.: The analysis of turbulence intensity based on wind speed data in onshore wind farms, *Renewable energy*, 123, 756–766, <http://dx.doi.org/10.1016/j.renene.2018.02.080>, 2018.
- 640 Robertson, A. N., Shaler, K., Sethuraman, L., and Jonkman, J.: Sensitivity analysis of the effect of wind characteristics and turbine properties on wind turbine loads, *Wind Energy Sci.*, 4, 479–513, <http://dx.doi.org/10.5194/wes-4-479-2019>, 2019.
- Rognin, F., Abdi, F., Kunc, V., Lee, M., and Nikbin, K.: Probabilistic methods in predicting damage under multi-stage fatigue of composites using load block sequences, *Procedia Eng.*, 1, 55–58, <http://dx.doi.org/10.1016/j.proeng.2009.06.015>, 2009.
- Ronold, K. O., Wedel-Heinen, J., and Christensen, C. J.: Reliability-based fatigue design of wind-turbine rotor blades, *Eng. Struct.*, 21, 645 1101–1114, [http://dx.doi.org/10.1016/S0141-0296\(98\)00048-0](http://dx.doi.org/10.1016/S0141-0296(98)00048-0), 1999.
- Schaff, J. R. and Davidson, B. D.: A strength-based wearout model for predicting the life of composite structures, ASTM special technical publication, 1285, 179–200, <http://dx.doi.org/10.1520/STP19928S>, 1997.
- Slot, R. M., Sørensen, J. D., Svenningsen, L., Moser, W., and Thøgersen, M. L.: Effective turbulence and its implications in wind turbine fatigue assessment, *Wind Energy*, 22, 1699–1715, <http://dx.doi.org/10.1002/we.2397>, 2019.
- 650 Srensen, J., D.: Reliability assessment of wind turbines, in: *Safety, Reliability, and Risk Analysis: Beyond the Horizon*, <http://dx.doi.org/10.1201/b15938-5>, 2015.
- Stensgaard, H. T., Svenningsen, L., Moser, W., Sørensen, J. D., and Thøgersen, M. L.: Wind climate parameters for wind turbine fatigue load assessment, *J. of Solar Energy Eng.*, 138, 031 010, <http://dx.doi.org/10.1115/1.4033111>, 2016a.
- Stensgaard, T. H., Svenningsen, L., Sørensen, J. D., Moser, W., and Thøgersen, M. L.: Uncertainty in wind climate parameters and their 655 influence on wind turbine fatigue loads, *Renewable Energy*, 90, 352–361, <https://doi.org/10.1016/j.renene.2016.01.010>, 2016b.
- Sndergaard, A. dL. and Jóhannsson, H. P.: Assessment of fatigue and extreme loading of wind turbines, M.S., Aalborg University, 2016.



- Toft, H. S. and Sørensen, J. D.: Reliability-based design of wind turbine blades, *Structural Safety*, 33, 333–342, <http://dx.doi.org/10.1016/j.strusafe.2011.05.003>, 2011.
- 660 Tsugawa, Y., Sakamoto, N., Kawasaki, S., Arakawa, C., and Iida, M.: Analysis of Wind Turbine Fatigue Loads for Proper Estimation of Offshore Turbulence Intensity, *EWEA Offshore 2015*, Copenhagen, 10-12 March 2015. POID:008.
- Türk, M. and Emeis, S.: The dependence of offshore turbulence intensity on wind speed, *J. of Wind Eng. and Ind. Aerodynamics*, 98, 466–471, <http://dx.doi.org/10.1016/j.jweia.2010.02.005>, 2010.
- Veers, P. S.: *Fatigue reliability of wind turbine components*, 1990.
- Veers, P. S.: Statistical considerations in fatigue, *Journal of Fatigue and Fracture*, 19, 295–302, <http://dx.doi.org/10.31399/asm.hb.v19.a0002369>, 1996.
- 665 Velarde, J., Kramhøft, C., Mankar, A., and Sørensen, J. D.: Uncertainty modeling and fatigue reliability assessment of offshore wind turbine concrete structures, *Int. J. of Offshore and Polar Eng.*, 29, 165–171, <http://dx.doi.org/10.17736/ijope.2019.il54>, 2019.
- Velarde, J., Mankar, A., Kramhøft, C., and Sørensen, J. D.: Probabilistic calibration of fatigue safety factors for offshore wind turbine concrete structures, *Eng. Struct.*, 222, 111 090, <http://dx.doi.org/10.1016/j.engstruct.2020.111090>, 2020.
- 670 Veldkamp, D.: *A probabilistic approach to wind turbine fatigue design*, EWEC, Milan, Italy, 2007.
- Wang, H., Barthelmie, R. J., Pryor, S. C., and Kim, H. G.: A new turbulence model for offshore wind turbine standards, *Wind Energy*, 17, 1587–1604, <http://dx.doi.org/10.1002/we.1654>, 2014.
- Yanan, C., Zhenand, S., and Shunhe, L.: Experimental study on fatigue behavior of composite laminate, *Acta Aeronautica et Astronautica Sinica*, 12, B643–B646, 1991.
- 675 Zaccone, M.: Failure analysis of helical springs under compressor start/stop conditions, *Practical Failure Analysis*, 1, 51–62, <https://doi.org/10.1007/BF02715198>, 2001.